Incorporation of lanthanides in alumina matrices by a sol–gel process employing heterometallic alkoxides, $M[Al(OPr^i)_4]_3$, as precursors

Chaitanya K. Narula,*[a] Willes H. Weber,[b] Jackie Y. Ying[c] and Lawrence F. Allard[d]

[a]*Chemistry Department, Ford Motor Co., P.O. Box 2053, MD 3083, Dearborn, MI 48121, USA*
[b]*Physics Department, Ford Motor Co., P.O. Box 2053, MD 3028, Dearborn, MI 48121, USA*
[c]*Department of Chemical Engineering, Massachusetts Institute of Technology, Cambridge, MA 02139, USA*
[d]*High Temperature Materials Laboratory, Oak Ridge National Laboratory, P.O. Box 2008, Oak Ridge, TN 37831, USA*

Spectroscopic studies of the hydrolysis of heterometallic alkoxides, $M[Al(OPr^i)_4]_3$, M = La, Ce, suggest that they do not dissociate during the early stages of hydrolysis. Gels from these heterometallic alkoxides can be prepared by two methods (i) direct hydrolysis in Pr^iOH, and (ii) peptization with acetic acid. Changes that occur in the structure and surface properties of gels during heat treatment are monitored by BET surface area measurements and X-ray powder diffraction (XRD) studies. No crystalline phase is observed below 500 °C in xerogels derived from $La[Al(OPr^i)_4]_3$ and $Ce[Al(OPr^i)_4]_3$ or their mixtures. The XRD of the gel derived from $La[Al(OPr^i)_4]_3$ shows diffraction peaks at 900 °C due to $LaAlO_3$. Cerium oxide starts to separate out at 600 °C in xerogels prepared from $Ce[Al(OPr^i)_4]_3$, and at 700 °C in xerogels prepared from mixtures of $La[Al(OPr^i)_4]_3$ and $Ce[Al(OPr^i)_4]_3$. Raman spectra of the gels prepared from the mixtures of $La[Al(OPr^i)_4]_3$ and $Ce[Al(OPr^i)_4]_3$ show that the CeO_2 crystallite sizes are >100 Å, and CeO_2, in fact, contains lanthanum in a mixed fluorite structure. High-resolution electron microscopy confirms that the lanthanum is part of the CeO_2 fluorite structure even in lanthanum rich areas. X-Ray photoelectron spectroscopic (XPS) analysis of the lanthanum containing gels, heated to 500 and 1000 °C, shows a peak at 836.5 eV for La $3d_{5/2}$, which could be due to the presence of M—O—Al type bridges in the samples. The contribution of μ''' in the Ce 3d peaks suggests that both oxides, CeO_2 and Ce_2O_3, are present in cerium containing gels. The presence of lanthanum does not affect the distribution of Ce^{III} and Ce^{IV} in our samples.

In recent years, the sol–gel process has received considerable attention as a method for preparing metal oxides.[1,2] Sol–gel processing allows control of microstructure and surface properties[3] and results in high purity materials. These benefits have led to new applications in thin films, coatings, monoliths, fiber technology and catalysis.[2] Metal alkoxides are commonly used as precursors for the preparation of high purity oxides. A natural extension of this approach would be to use heterometallic alkoxides in the preparation of multicomponent oxides although they have not been extensively employed in sol–gel processing.[4,5] This is not surprising because it was believed that heterometallic alkoxides would disproportionate into their component alkoxides during hydrolysis.[6] When our work was initiated,[7,8] there were only two related reports in the literature. Mehrotra[9] briefly mentioned the hydrolysis studies on $Zr(OPr^i)_2[Al(OPr^i)_4]_2$ in a review and Jones *et al.*[10] described the preparation of magnesium aluminate spinel from $Mg[Al(OR)_4]_2$. Recently, Rai and Mehrotra discussed the hydrolysis of $Mg[Al(OR)_4]_2$ and $Ca[Al(OR)_4]_2$ in the absence of chelates.[11,12]

Our interest in heterometallic alkoxides as precursors is a continuation of our efforts in developing a variety of automotive applications of sol–gel processed alumina- and silica-based materials. We have previously shown that thin layers of conducting metal oxides can be employed in designs for electrically heated catalyst devices,[13] on-board diagnostic devices,[14] and calorimetric sensor devices.[15] Replacing commercial alumina with a sol–gel processed, controlled pore-size alumina in lean-burn NO_x reduction catalyst formulations improved the activity of the catalyst by 30%.[16] We also found that a 10% loading of sol–gel processed alumina as washcoat furnished a surface area equal to that of a commercial catalyst (33% loading of washcoat) resulting in open channels and a reduced back-pressure problem.[17]

Commercial alumina-based washcoats generally contain lanthanides (La_2O_3 2–3%, CeO_2 20%) and alkaline earths (BaO 2–3%) which contribute towards the stabilization of alumina at elevated temperatures, the enhancement of the activity of the noble metals and provide improved oxygen storage capacity.[18,19] Cerium oxide in alumina is believed to improve catalyst performance by easily undergoing partial reduction and oxidation, thereby buffering the effects of air-to-fuel ratio fluctuations.[20] A recent study suggests that La^{3+} incorporation in alumina prior to CeO_2 addition improves the dispersion of CeO_2 and provides a greater range of reversible reducibility,[21] which increases the activity of three-way automotive catalysts (TWC).[22]

The incorporation of lanthanides in alumina is generally carried out by treating commercial alumina with nitrates of lanthanides, then heating to decompose the nitrates to oxides.[18] Although the preparation of lanthanum aluminate by a sol–gel process using a mixture of lanthanum alkoxide and aluminium alkoxides is known, this method has not been employed in the preparation of catalyst materials.[19] In our investigations, we selected heterometallic alkoxides since a substantial loss of yield occurs during the purification of $Ln(OR)_3$.[23,24] Heterometallic alkoxides, $M[Al(OPr^i)_4]_3$, M = La, Ce, can be prepared in high yields and purity. Furthermore, heterometallic alkoxides, $M[Al(OPr^i)_4]_3$, form in a solution of $M(OPr^i)_3$ and $Al(OPr^i)_3$.

Here, we describe our studies to incorporate lanthanides in alumina by the sol–gel process using heterometallic alkoxides, $M[Al(OPr^i)_4]_3$ (M = La, Ce), as precursors. The spectroscopic analysis of partially hydrolyzed $M[Al(OPr^i)_4]_3$ supports observations, by other workers, that the precursors do no dissociate at the early stages of hydrolysis. The gels prepared from these precursors are amorphous and form crystalline materials at high temperatures. We present X-ray diffraction, Raman and electron microscopic studies on the structural changes that occur on thermal treatment of the gels. The surface analysis (XPS) of thermally treated gels is also discussed.

Experimental

All experiments were carried out in an inert atmosphere using standard vacuum line techniques to avoid hydrolysis of the alkoxides on contact with atmospheric humidity. Propan-2-ol was dried over $NaOPr^i$ before use. Commercial $Al(OPr^i)_3$ was distilled to remove oxide impurities. Heterometallic alkoxides, $La[Al(OPr^i)_4]_3$ and $Ce[Al(OPr^i)_4]_3$, were prepared by the reaction of $LaCl_3{\cdot}3Pr^iOH$ or $CeCl_3{\cdot}3Pr^iOH$ with $K[Al(OPr^i)_4]$.[24–26]

The NMR spectra were recorded on a Bruker WM-360 instrument. Thermogravimetry was carried out on a Perkin-Elmer TA7 instrument. The X-ray powder diffraction data were collected on a Scintag diffractometer. BET surface areas were measured on a Micromeritics ASAP2400 instrument. Raman spectra were recorded using a SPEX Triplemate spectrometer, an intensified diode array detector system, and an Ar^+-ion laser. IR and photoacoustic IR spectra of the samples were obtained on a Perkin-Elmer FT2000 IR instrument. The X-ray photoelectron spectra of thermally treated gels were recorded on a Perkin-Elmer PHI5400 machine. Images and energy dispersive X-ray analyses were obtained using a Hitachi HF-2000 field emission transmission electron microscope equipped with a Noran ultra-thin-window detector system.

General method for the preparation of gels

Direct hydrolysis. A clear solution was obtained when $La[Al(OPr^i)_4]_3$, $Ce[Al(OPr^i)_4]_3$, or their 1:1 or 1:3 mixtures in propan-2-ol were reacted with water mixed in propan-2-ol at −78 °C. Gels formed on slowly warming the reaction mixture to room temperature. Volatiles were removed in vacuum to obtain xerogels.

Peptization method. Sols from $La[Al(OPr^i)_4]_3$, $Ce[Al(OPr^i)_4]_3$, or their 1:1 or 1:3 mixtures were prepared by adding their solutions in dry propan-2-ol to water at 80 °C with stirring. The reaction mixture was heated to 90 °C to boil off propan-2-ol, and a few drops of glacial acetic acid added to obtain an almost clear sol. A cation to acetic acid ratio of *ca.* 1:1 is sufficient and excess acetic acid does not significantly change the peptization time. The sol was gently refluxed for 16 h.

Results and Discussion

We initiated our work by carrying out a spectroscopic study of the partially hydrolyzed $M[Al(OPr^i)_4]_3$, M = La and Ce. This was followed by the preparation of sols and gels by direct hydrolysis and peptization methods employing $La[Al(OPr^i)_4]_3$, $Ce[Al(OPr^i)_4]_3$ and their mixtures. The dried gels were examined by X-ray powder diffraction for structural changes as a function of temperature. In the samples containing both lanthanum and cerium oxide, the dissolution of lanthanum in cerium oxide could not be reliably determined by shifts in the $CeO_2(311)$ diffraction peak due to small particle size. Therefore, we relied on the Raman scattering and high resolution electron microscopy to obtain evidence of the dissolution of lanthanum oxide in cerium oxide. We also analyzed the surface chemical state of cerium oxide by X-ray photoelectron spectroscopy.

Spectroscopic study of partially hydrolyzed $La[Al(OPr^i)_4]_3$ and $Ce[Al(OPr^i)_4]_3$

The precise mechanism of the hydrolysis of heterometallic alkoxides remains to be determined, although scattered information has appeared in the literature. Hirano *et al.* suggested the loss of bridging alkoxy groups, based on their IR study of partially hydrolyzed heterometallic alkoxides.[27] Recent work by Caulton and co-workers,[28] Payne and co-workers,[29] and Hubert-Pfalzgraf[5] suggested that disproportionation of heterometallic alkoxides does not occur at the early stages of hydrolysis, supporting the earlier suggestions by Mehrotra,[9] Caulton and co-workers[28] described the X-ray structure of the partial hydrolysis products of $Li_2Ti_2(\mu_3\text{-}OPr^i)_2(\mu\text{-}OPr^i)_4(OPr^i)_4$ and $BaZr_4(OPr^i)_{18}$. The resulting compounds $Li_4Ti_4(\mu_5\text{-}O)_2(\mu\text{-}O)_2(\mu_3\text{-}OPr^i)_4(\mu\text{-}OPr^i)_4(OPr^i)_2$ and $BaZr_4(OH)(OPr^i)_{17}$ contain Li—O—Ti and Ba—OH—Zr linkages respectively showing that the hydrolysis of heterometallic alkoxides could proceed either by preferential attack on bridging alkoxides, as in Ba–Zr alkoxides, or by attack on both bridging and terminal groups, as in Li–Ti alkoxide. This observation is different from Mehrotra's suggestion that the hydrolysis of heterometallic alkoxides is a two step process, first a transient species is formed with the replacement of terminal alkoxy groups by hydroxy groups which rearranges to compounds with bridging hydroxy groups. Our results on ^1H NMR study of systematic hydrolysis of $La[Al(OPr^i)_4]_3$ provide some support to this hypothesis.

We carried out the reactions of $M[Al(OPr^i)_4]_3$ (M = La, Ce) with water in propan-2-ol in 1:1 to 1:7 ratios at −78 °C to ensure uniform mixing. The reaction products are designated La_{11}–La_{17} and Ce_{11}–Ce_{17}, where the subscripts show the ratio of alkoxide to water. The reaction products La_{11}–La_{16} are soluble in propan-2-ol and the reaction product La_{17} is a gel. All compounds show a broad strong peak in their IR spectra at 3500 cm^{-1} due to the presence of hydroxy groups. The products La_{11}, La_{12} and La_{13} isolated after heating the reaction mixture under reflux do not show this peak, suggesting the loss of hydroxy groups.

Although the ^1H NMR spectra of these compounds are too complex to determine structural details, an interesting trend can be seen (Fig. 1) as the degree of hydrolysis increases. The ^1H NMR spectrum of the precursor, $La[Al(OPr^i)_4]_3$, is quite simple and exhibits a doublet at 1.23 ppm for CH_3 proton and a septet at 4.24 ppm for CH protons. The ^1H NMR spectrum of the soluble fraction becomes increasingly complex as the degree of hydrolysis increases from La_{11} to La_{13}. The spectrum simplifies as more OPr^i groups are replaced and finally La_{16} shows a doublet for CH_3 and a multiplet for CH protons. This pattern can be explained by assuming that bridging groups are replaced preferentially. Thus replacement of one bridging OPr^i group creates an asymmetrical structure. The second OH group can occupy any of the residual five positions resulting in symmetrical and asymmetrical structures involving $(OH)_2Al(OPr^i)_2$ or $(OH)(OPr^i)Al(OPr^i)_2$ ligands. These in turn can occupy the *cis*- or *trans*-position to $(OPr^i)_2Al(OPr^i)_2$ ligands.

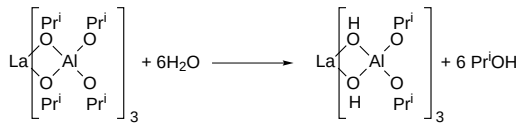

The structure becomes more complicated with the replacement of a third OH group. A simpler structure results after the replacement of all six bridging OPr^i ligands with OH groups because these groups create a symmetrical environment of $(OH)_2Al(OPr^i)_2$ ligands around lanthanum.

These results seem to support Mehrotra's suggestion that the replacement of bridging OPr^i groups by OH groups should be observed in the hydrolysis products of heterometallic alkoxides.[9] However, if this model is correct, the IR spectra of the La_{11} through La_{15} should show the reduction in peak intensity due to bridging OPr^i groups relative to the terminal OPr^i groups and the IR spectra of La_{16} should exhibit complete absence of bridging OPr^i groups. A comparison of the IR spectrum of La_{16} with that of $La[Al(OPr^i)_4]_3$ shows them to be identical in the 1600–900 cm^{-1} range [bridging and terminal ν(C—OM) are present in this region]. This suggests that

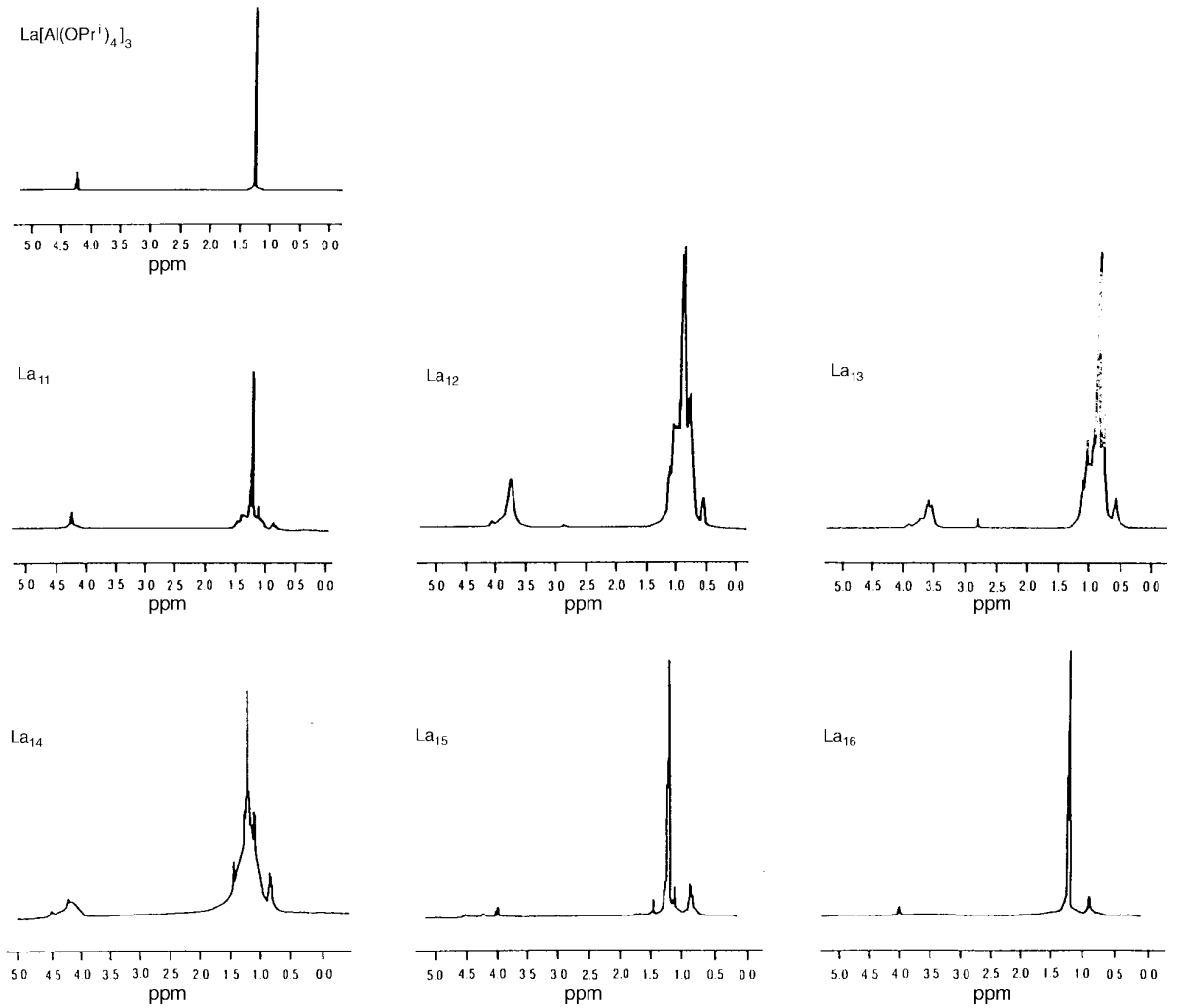

Fig. 1 ^{1}H NMR spectra of partially hydrolyzed La[Al(OPr^i)$_4$]$_3$

Mehrotra's model might apply to soluble species only and bulk La_{16} is a mixture of compounds and the La—OH—Al bridges are probably present at least in the early stages of hydrolysis. The ^{1}H NMR spectra of the species isolated from hydrolysis reactions of Ce[Al(OPr^i)$_3$]$_4$ are quite complex, probably due to a large number of structures formed as the result of hydrolysis and the oxidation of Ce^{III} to Ce^{IV}.

Thermal treatment of gels

Gels derived from La[Al(OPr^i)$_4$]$_3$. *Direct hydrolysis.* Removal of the solvent under vacuum furnishes xerogels as granular solids. The data described here are from gels prepared by treatment with 12 equivalents of water. We find it necessary to use excess water in preparation of gels to reduce residual alkoxy groups, otherwise the gels turn black during pyrolysis at *ca.* 600 °C and lose surface area rapidly on firing at 900 °C. Thermogravimetry (TG) of the xerogels in air shows a mass loss of 25% in the temperature range 50–250 °C and 5% in the range 250–400 °C. No further mass loss is observed in the range 400–900 °C. After a gel sample was heated to 400 °C and maintained at that temperature for 8 h, the BET surface area of the resulting powder was determined to be 221 $m^2\ g^{-1}$. X-Ray powder diffraction (XRD) showed no diffraction peaks, suggesting that it was amorphous. After sintering at 500 °C, analysis of the gel showed two very weak, broad peaks centered at $2\theta = 30$ and 45° [Fig. 2(a)]. The crystallization of $LaAlO_3$ (JCPDS no. 31–22) takes place at 900 °C [Fig. 2(b), average

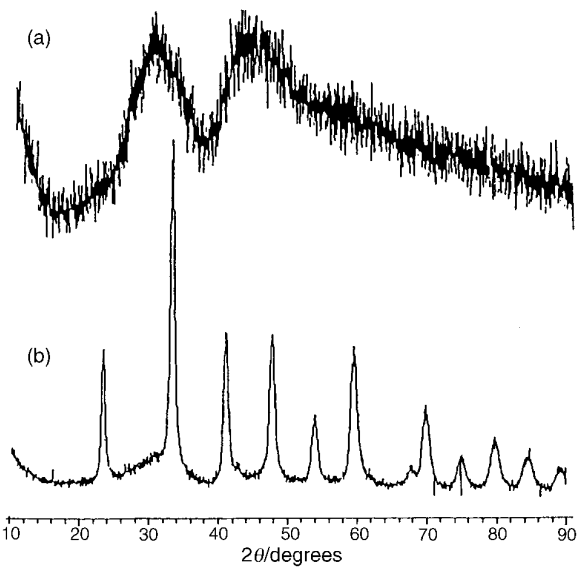

Fig. 2 XRD patterns of La[Al(OPr^i)$_4$]$_3$ gels heated to (a) 500 °C and (b) 900 °C

grain size >15 nm from Scherrer formula]. There is a broad, weak peak at $2\theta = 67°$ which is probably as a result of the initiation of crystallization of γ-alumina (JCPDS no. 10–425), although two equivalents of alumina remain amorphous. The gels were also characterized by photoacoustic (PA)-FTIR spectroscopy. The PA-FTIR spectrum of the dry gel is presented in Fig. 3(a). The high surface area sample gave rise to a broad IR absorption between 3000 and 3600 cm^{-1} due to H-bonded O—H stretching.[30] The features at 2825–2950 cm^{-1} are assigned to C—H stretching from adsorbed hydrocarbons and residual alkoxy groups. The features at 1515 and 1390 cm^{-1} are attributed to adsorbed carbonates. The phonon vibrations of metal oxide begin to absorb strongly below 1200 cm^{-1}, similar to γ-Al_2O_3.[30,31] Upon heat treatment to 1000 °C, the molecular structure of the gel remained very similar to that of pure γ-Al_2O_3.[30,31] A decrease in surface area after the high-temperature treatment presented diminished absorptions of H-bonded OH and adsorbed carbonate in the PA-FTIR spectrum [Fig. 3(b)]. The phonon absorption below 1100 cm^{-1} did not give us distinct features from the presence of La in alumina. La—O—Al may well have overlapped with Al—O—Al lattice vibrations in this broad absorption band.

Peptization method. Peptization of hydrolyzed $La[Al(OPr^i)_4]_3$ at 80 °C with acetic acid furnished a sol which formed a transparent gel on evaporation of the volatiles. The gel was dried at 100 °C, collected, and powdered. A mass loss of 30% in 50–300 °C range was observed in TG, and no further mass loss was observed in the temperature range 300–900 °C.

The gel was heated in 100 °C increments between 500–900 °C with an 8 h holding period at each temperature. The BET surface area [Fig. 4(a)] decreased slowly as the gel was treated at higher temperatures and was found to be 40 $m^2\ g^{-1}$ after treatment at 900 °C. The materials remained amorphous at 700 °C and crystallization took place at 900 °C with the separation of only $LaAlO_3$ while the other two equivalents of alumina remained amorphous.

Gels derived from $Ce[Al(OPr^i)_4]_3$. *Direct hydrolysis.* The gel, prepared from the reaction with excess water, showed a 30% mass loss in the 50–380 °C temperature range and no subsequent mass loss in the 400–900 °C range during TG in air. Pyrolysis of this light yellow gel at 400 °C in air for 8 h left a yellow amorphous powder with a BET surface area of 213 $m^2\ g^{-1}$. This powder was heated in 100 °C increments between 500 and 900 °C with an 8 h holding period at each temperature. The BET surface area [Fig. 4(b)] decreased during this heat treatment and the powder remained amorphous up to 500 °C. Poorly crystalline cerium oxide (average grain size *ca.* 2 nm from the Scherrer formula) started to develop upon heating at 600 °C with broad diffraction peaks [Fig. 5(a)]. On subsequent heating to 900 °C, the crystallite size remained very small (*ca.* 15 nm from the Scherrer formula) [Fig. 5(b)]. There is a broad weak peak at $2\theta = 67°$ which is probably due to the initiation of crystallization of γ-alumina (JCPDS no. 10–425). However, the bulk of the alumina remains amorphous during this heat treatment.

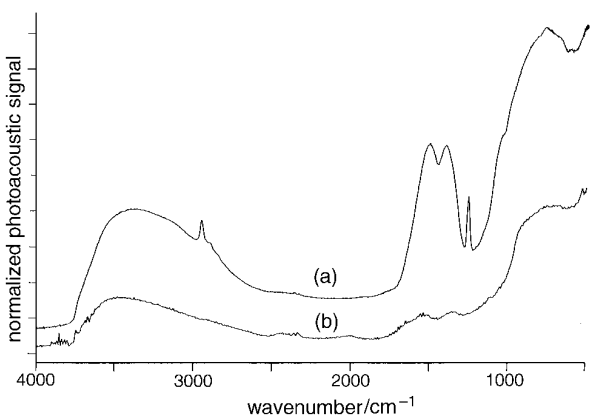

Fig. 3 PA-FTIR spectra of $La[Al(OPr^i)_4]_3$ gels (a) as-prepared and (b) after heat treatment to 1000 °C

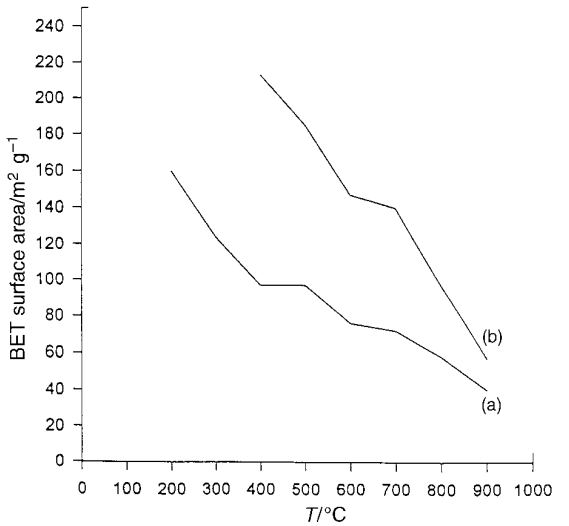

Fig. 4 BET surface areas of gels derived from (a) $La[Al(OPr^i)_4]_3$ and (b) $Ce[Al(OPr^i)_4]_3$ after thermal treatment at the given temperature

Peptization method. The sol, prepared by peptization of hydrolysis products of $Ce[Al(OPr^i)_4]_3$ with acetic acid, was converted to gel and finally to xerogel by evaporation of solvent from heating at 100 °C. A mass loss of 30% was seen in TG in the temperature range 50–250 °C. After pyrolysis at 400 °C for 4 h, an amorphous powder with a BET surface area of 192 $m^2\ g^{-1}$ was obtained.

Gels derived from mixtures of $La[Al(OPr^i)_4]_3$ and $Ce[Al(OPr^i)_4]_3$. We prepared La–Ce–Al–O gels by co-

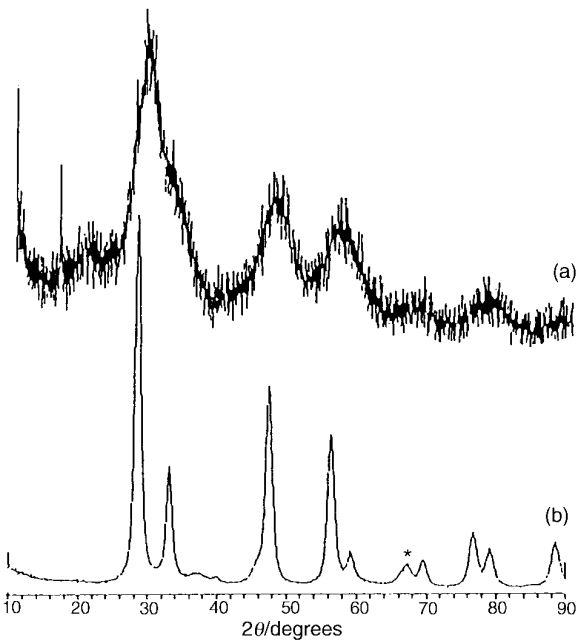

Fig. 5 XRD patterns of $Ce[Al(OPr^i)_4]_3$ gels heated to (a) 600 °C and (b) 900 °C (* indicates peak due to γ-Al_2O_3)

hydrolysis of $La[Al(OPr^i)_4]_3$ and $Ce[Al(OPr^i)_4]_3$ in 1:1 and 1:3 ratios, designated $LaCeAl_{11}$ and $LaCeAl_{13}$, respectively (subscript shows the ratio of alkoxides). TG of both gels, $LaCeAl_{11}$ and $LaCeAl_{13}$, in air showed a mass loss of 30% in the region 50–400 °C and none in the region 400–900 °C.

After heating $LaCeAl_{11}$ in air at 550 °C for 4 h an amorphous yellow solid with a BET surface area of 159 $m^2\ g^{-1}$ was obtained. The XRD pattern showed CeO_2 diffraction peaks after heating at 900 °C [Fig. 6(a)]. After heating the $LaCeAl_{13}$ gel at 550 °C for 5 h, the material was amorphous and had a BET surface area of 164 $m^2\ g^{-1}$. The XRD pattern showed weak, broad CeO_2 diffraction peaks after heating at 700 °C; these peaks became better defined after heating at 900 °C [Fig. 6(b)] (average grain size 4–5 nm from the Scherrer formula). The alumina and lanthanum oxide components of both $LaCeAl_{11}$ and $LaCeAl_{13}$ gels remained amorphous even after heating at 900 °C.

The extent of lanthanum doping in cerium oxide in $LaCeAl_{11}$ and $LaCeAl_{13}$ could not be reliably determined by shifts in the $CeO_2(311)$ diffraction peaks, which are very broad owing to small grain size. The results of both Raman scattering and electron microscopy suggest that the X-ray powder diffraction pattern observed for $LaCeAl_{11}$ and $LaCeAl_{13}$ should be assigned to $Ce_{1-x}La_xO_{2-y}$.

Raman spectroscopy

Cerium dioxide has a single allowed Raman mode, which occurs at 465 cm^{-1} in pure materials. McBride *et al.* have shown that in mixed crystals of the form $Ce_{1-x}La_xO_{2-y}$ there is a systematic downward shift of this frequency with increasing La concentration.[32] The lattice constant also increases with La concentration, as shown by earlier XRD work. Such crystals maintain the fluorite structure with the La content as high as 50%.[33] It is thus possible to deduce the fraction of La incorporated into the CeO_2 lattice from a measurement of the frequency shift.

Raman spectra were obtained from $LaCeAl_{11}$ and $LaCeAl_{13}$ samples using a SPEX Triplemate spectrometer, an intensified diode array detector system, and an Ar^+-ion laser. The laser power was kept low (*ca.* 2 mW) to avoid sample heating, since small changes in temperature can produce small changes in the frequency and width of the Raman line. Similar small changes in the Raman line can result from small particle effects if the crystallite sizes are *ca.* 10 nm or less.[34,35] We therefore fired the samples also at 1200 °C in order to increase the particle size. The resulting spectra had peak frequencies of 460.2 and 459.4 cm^{-1} and widths (half-width at half-maximum) of 7.6 and 8.9 cm^{-1}, for the $LaCeAl_{11}$ and $LaCeAl_{13}$ (Fig. 7) samples, respectively. From the observed widths we conclude that the crystallite sizes are >10 nm, and from the peak frequencies that the La concentration in the mixed fluorite-structure crystal is 10–15%. However, electron microscopic studies, described below, suggest that the fluorite structure is retained even when the lanthanum concentration is higher than cerium.

These data also suggest that lanthanum preferentially reacts with CeO_2 over Al_2O_3 explaining the absence of $LaAlO_3$ in $LaCeAl_{11}$ and $LaCeAl_{13}$, which was the only crystalline phase observed in gels derived from $La[Al(OPr^i)_4]_3$. The Raman results confirm the absence of La_2O_3, which has an easily recognized Raman signature, and of $CeAlO_3$, which tends to produce a strong fluorescence background.[36]

High-resolution electron microscopy

We selected three samples, LaAl/1000, CeAl/1000, and LaCeAl/1000 for high-resolution electron microscopic studies because these samples contain crystalline phases. Fig. 8(a) shows a low magnification micrograph of LaAl/1000 samples in which agglomerates of *ca.* 250–300 nm size can be seen. The energy dispersive spectra (EDS) of several individual particles exhibited lanthanum peaks. The high resolution electron micrograph [Fig. 8(b)] shows an amorphous particle with a crystalline zone. The crystalline zone is *ca.* 10 nm in size and exhibits $LaAlO_3(111)$ lattice fringes (JCPDS no. 31–22). These were measured from a Fast Fourier Transform (FFT), appropriately calibrated, taken from the structure. These data are commensurate with the X-ray powder diffraction data which also suggested the crystallites of size 12 nm.

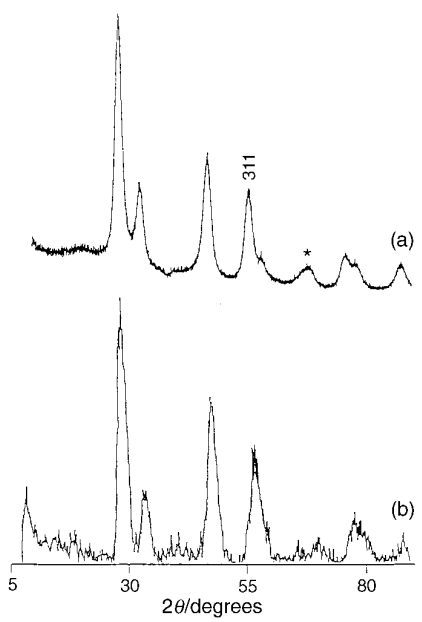

Fig. 6 XRD patterns of (a) $LaCeAl_{11}$ and (b) $LaCeAl_{13}$ heated to 900 °C (* indicates peak due to γ-Al_2O_3)

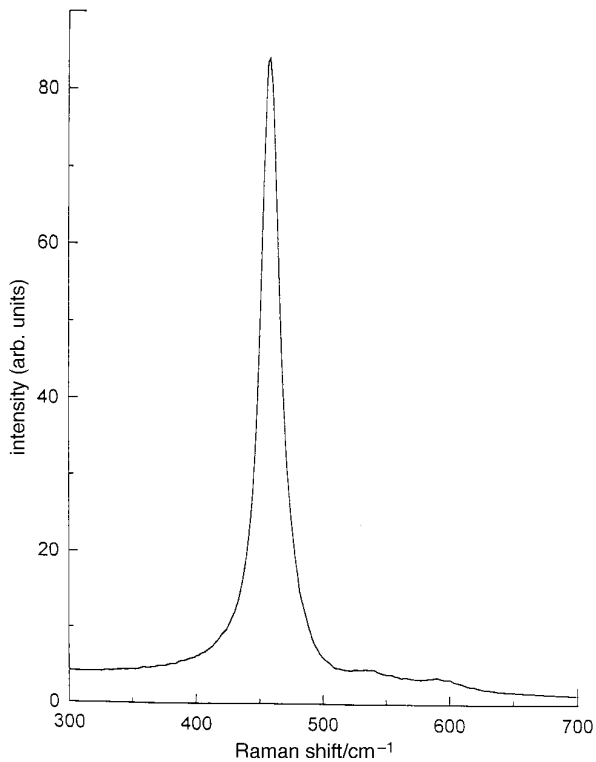

Fig. 7 Raman spectrum of $LaCeAl_{13}$ powder obtained using the 457.9 nm laser line after sintering the sample at 1200 °C

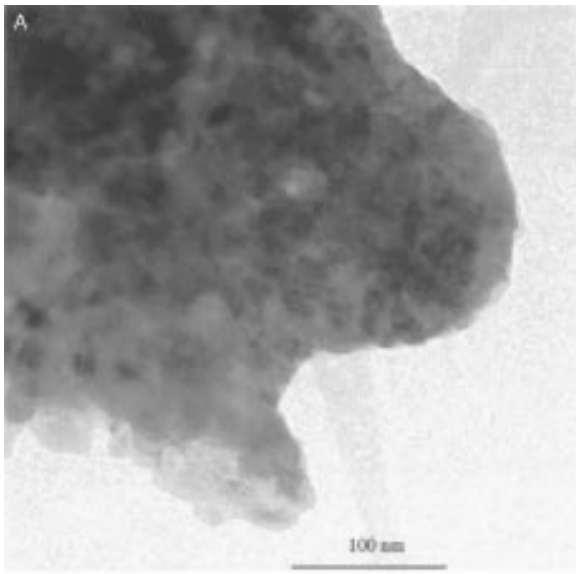

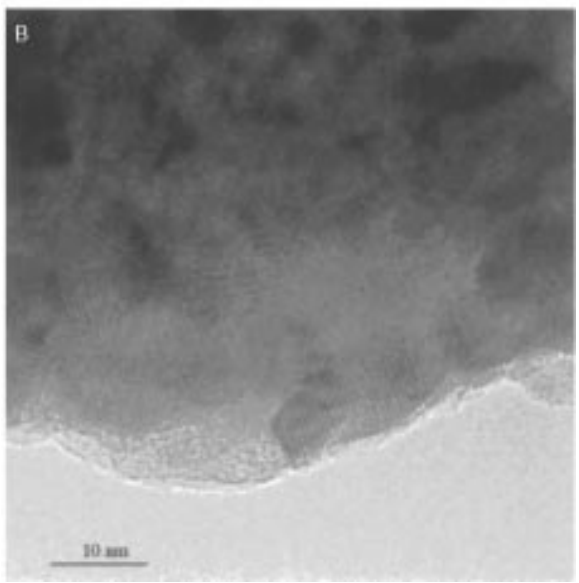

Fig. 8 Transmission electron micrographs of LaAl/1000. A, The image shows it to be an agglomerate of small particles. B, HREM image shows (111) lattice fringes for $LaAlO_3$.

The TEM of CeAl/1000 at low magnification shows particles to be 80–100 nm agglomerates. EDS shows an even distribution of cerium, aluminium and oxygen in these agglomerates. High-resolution micrographs (Fig. 9) show crystalline zones with lattice fringes corresponding to CeO_2(111).

The high-resolution electron micrograph of $LaCeAl_{11}$/1000 shows an amorphous particle with a small crystalline zone where Al_2O_3(311) fringes can be seen [Fig. 10(a)]. This suggests that the crystallization of alumina has initiated. There is also a crystalline area near the edge of the particle. EDS of the crystalline area shows the presence both lanthanum and cerium in varying ratio. The area marked on Fig. 10(a) as La,Ce exhibits an equal ratio of lanthanum and cerium whereas the areas marked La and Ce show an excess of lanthanum and cerium respectively. The high resolution electron micrographs of all three regions [Fig. 10(b)–(d)] exhibit lattice fringes which correspond to CeO_2(111). Thus the fluorite structure is retained regardless of the concentration of lanthanum. These observations confirm the results from Raman scattering that lanthanum preferentially dissolves in the cerium oxide matrix.

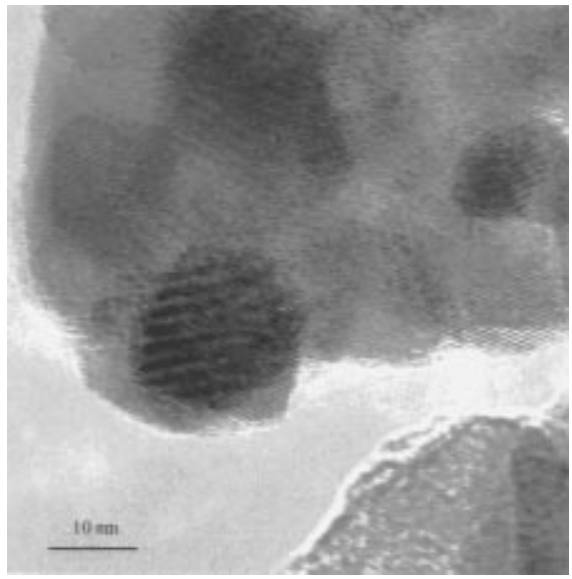

Fig. 9 HREM image of CeAl/1000. The micrograph shows (111) lattice fringes for CeO_2.

X-Ray photoelectron spectroscopic analysis of gels

XPS has been employed by several authors to determine the surface structures of lanthanide impregnated aluminas which are commonly employed in high temperature catalysis.[18,21,37,38] The XPS of lanthanum and cerium oxides is quite complex owing to the presence of satellites. This is further complicated for cerium oxides because the $3d_{5/2}$ and $3d_{3/2}$ core level spectra show six and four separate contributions from Ce^{3+} and Ce^{4+} respectively. Despite the complex nature of the spectra, they have been used to determine the ratio of Ce^{3+} and Ce^{4+} in the cerium oxide samples.[21] In addition, the presence of lanthanum oxides has been shown to influence the oxidation state of cerium oxide.[21]

For this study, we selected representative gels LaAl/500, LaAl/1000, CeAl/500, CeAl/1000, $LaCeAl_{11}$/500, and $LaCeAl_{11}$/1000 where /*n* denotes the calcination temperature (°C). The binding energy of adventitious C 1s peaks (284.8 eV) has been used as an internal reference to correct for charging in some of the samples. A second C 1s peak with binding energy of 283 eV, arising from trace amounts of carbides, can also be resolved. Deconvolution of peaks was performed using peakfit program from Jandel Scientific. The standard deviation of binding energies is in the range 0.02–0.07 eV.

The Al 2p peaks for LaAl/500 were at 74.0 and 72.8 eV; these peaks are due to boehmite and γ-alumina.[39] Thermal treatment simplifies the Al 2p window and only one peak at 73.6 eV is observed in LaAl/1000 [Fig. 11(a)]. The effect of lanthanum on alumina is not seen, which is not surprising since the binding energy of compounds such as $LaAlO_3$,[40] $CuAl_2O_4$,[41] $Al_2(WO_4)_3$,[42] and α-Al_2O_3,[39] have been reported to be 72.4, 74.2, 74.7 and 73.8 eV suggesting that Al 2p of lanthanum aluminate cannot be easily resolved. The cerium-containing sample CeAl/500 also showed two Al 2p peaks at 73.9 and 72.4 eV due to boehmite and γ-alumina. However, the high-temperature sample CeAl/1000 shows peaks at 74.5, 73.3 and 71.9 eV in 3 : 5 : 2 ratio [Fig. 11(b)]. The peaks at 74.5 and 71.9 eV are probably due to the interaction of cerium with alumina. The mixed sample, $LaCeAl_{11}$/500, exhibited peaks at 75.2, 73.8 and 72.4 eV in 2 : 5 : 3 ratio. The higher temperature sample $LaCeAl_{11}$/1000 shows only two peaks at 73.6 and 72.2 eV in 1 : 1 ratio.

The O 1s window of LaAl/500 and LaAl/1000 showed three peaks at 532.1, 530.5, 529.1 and 532.6, 531.3, 530 eV, respectively [Fig. 12(a)]. The middle peak (*ca.* 531 eV) is due to

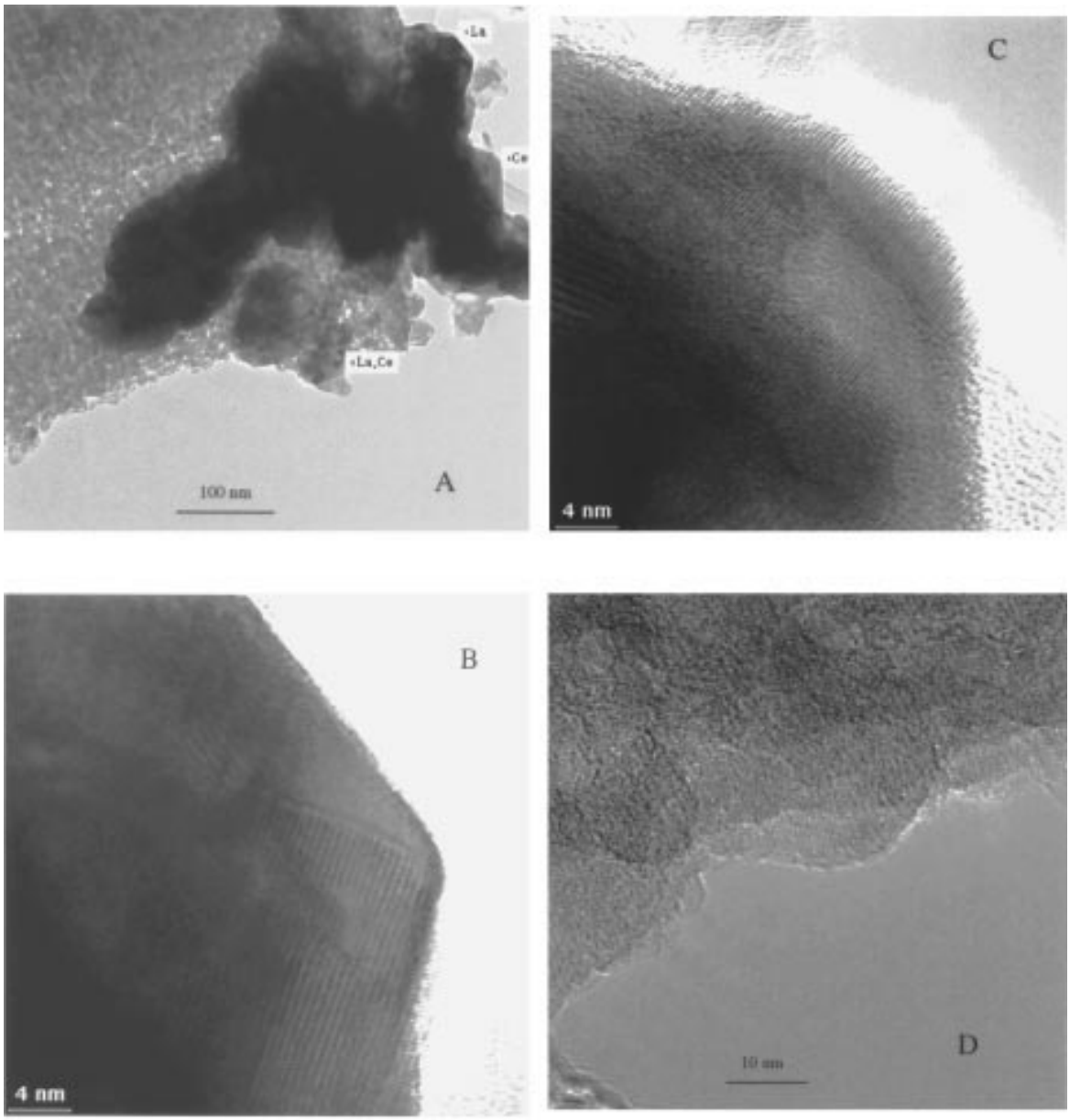

Fig. 10 A, TEM of $LaCeAl_{11}/1000$. B, HREM of area marked La. C, HREM of area marked Ce. D, HREM of area marked La,Ce. Micrographs B, C and D show (111) lattice fringes for CeO_2 lattice.

alumina[43] and the other two peaks (*ca.* 3 eV apart) are due to lanthanum oxide.[44] The binding energy of O 1s of $LaAlO_3$ single crystal is reported to be 529 eV, suggesting that O 1s due to La—O—Al interaction in our sample will overlap with La_2O_3 peak. The CeAl/500 also showed three peaks at 531.9, 529.4 eV for cerium oxide and 530.2 eV for alumina.[43,44] The higher temperature sample CeAl/1000 showed three peaks at 531.6 and 528.5 for cerium oxide and 530.1 eV for alumina [Fig. 12(b)].

Both LaAl/500 and LaAl/1000 exhibited La $3d_{5/2}$ at 835.1 eV assignable to La_2O_3[44] (Fig. 13). The binding energy of La $3d_{5/2}$ is reported[40] to be 834.5 eV and is not resolved in our sample. A second peak at 836.9 eV close to the lanthanum oxalates and sulfates (837.0 3V) was also observed.[44] This peak has previously been assigned to 'dispersed phase' lanthanum oxide[37] but could be due to lanthanum bonded to aluminium through oxygen bridges since such species would have cationic lanthanum. At least two sets of peaks are also present in the La 3d window of $LaCeAl_{11}/500$ and $LaCeAl_{11}/1000$ at energies which are lower by 2.5 eV. This suggests that the structure of $LaCeAl_{11}$ materials is different from that of LaAl materials.

The Ce 3d window of the samples CeAl/500, CeAl/1000, $LaCeAl_{11}/500$ and $LaCeAl_{11}/1000$ showed several peaks (Fig. 14 and 15). Although these peak positions have been determined by fitting the peaks, the peak positions should not be taken as absolute values. The difficulty in fitting the peaks for cerium oxides has also been previously noted.[44] It is, however, possible to calculate the approximate ratio of Ce^{III} and Ce^{IV} from the contribution of μ''' (*ca.* 917 eV) towards the total area of the Ce 3d.[21] The values for pure CeO_2 and Ce_2O_3 are 14 and 2%, respectively. The contributions of μ''' for CeAl/500, CeAl/1000, $LaCeAl_{11}/500$, and $LaCeAl_{11}/1000$ are 9.27, 10.84, 9.4 and 12.6%, respectively. The presence of lanthanum does not seem to influence the stabilization of cerium in oxidation state +4 over +3. We note that only a CeO_2 and not a Ce_2O_3 phase was detected in the XRD patterns, indicating that cerium oxide is present as an oxygen-deficient CeO_{2-x} phase.

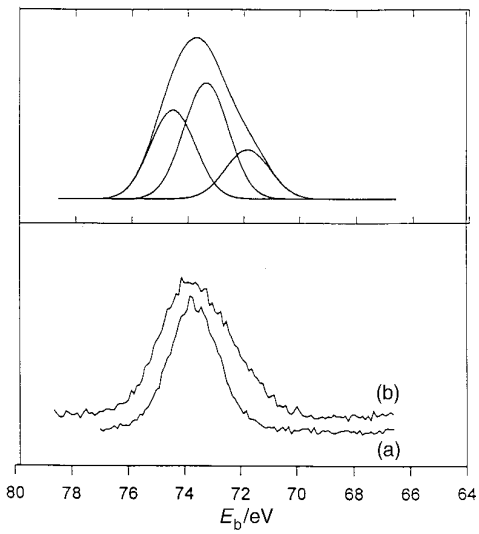

Fig. 11 Al 2p spectra of (a) LaAl/1000 and (b) CeAl/1000

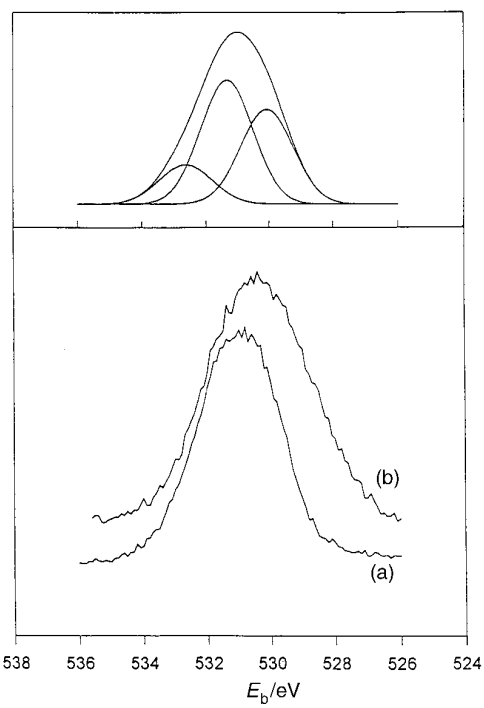

Fig. 12 O 1s spectra of (a) LaAl/1000 and (b) CeAl/1000

The XPS studies illustrate that the surfaces of cerium-containing materials have cerium in both +3 and +4 oxidation states. The samples containing both lanthanum and cerium oxides show no influence of lanthanum oxides on the ratio of the cerium in +3 and +4 oxidation states. The data also provide some evidence for the presence of La—O—Al bridges in LaAl/500 and $LaCeAl_{11}$/500, which are amorphous materials.

Conclusions

Heterometallic alkoxides, $M[Al(OPr^i)_4]_3$ (M = La, Ce), furnish gels with a fine distribution of lanthanides in alumina. Separation of lanthanide oxide occurs at elevated temperatures. The gels derived from $La[Al(OPr^i)_4]_3$ form $LaAlO_3$ (average grain size *ca.* 15 nm) at 900 °C and those from $Ce[Al(OPr^i)_4]_3$ form CeO_2 (average grain size *ca.* 15 nm) at 900 °C. The grain

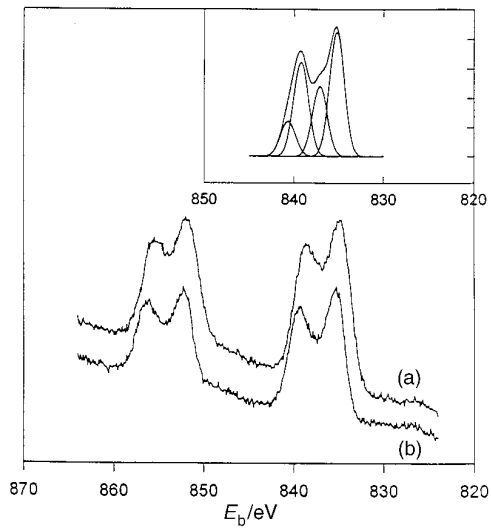

Fig. 13 La 3d spectra of (a) LaAl/500 and (b) LaAl/1000

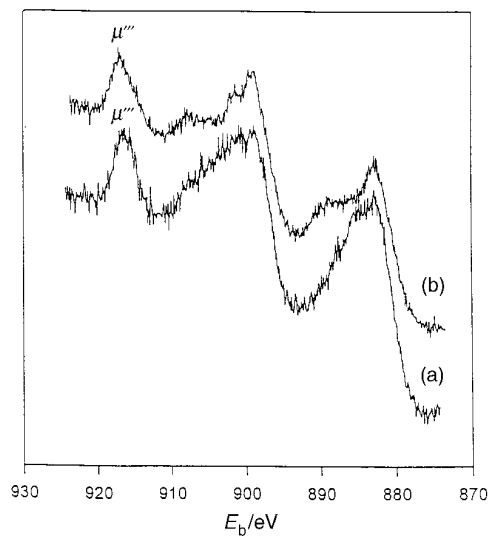

Fig. 14 Ce 3d core-level spectra of (a) CeAl/500 and (b) CeAl/1000

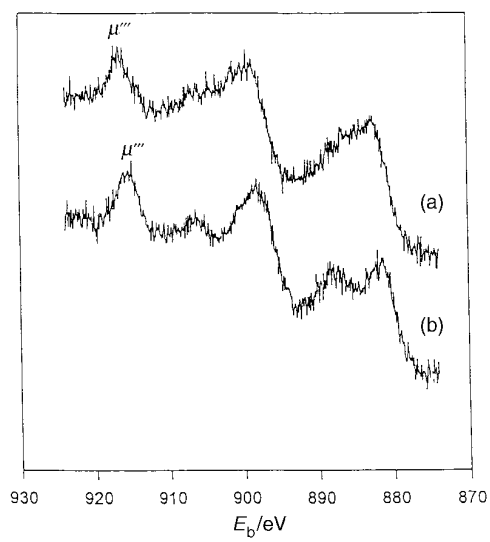

Fig. 15 Ce 3d core-level spectra of (a) $LaCeAl_{11}$/500 and (b) $LaCeAl_{11}$/1000

size of crystalline phases in $LaCeAl_{11}$ and $LaCeAl_{13}$ remains in the 10–15 nm range even after heating to 1200 °C with fluorite-structure crystallites of $Ce_{1-x}La_xO_{2-y}$. Alumina remains amorphous in all CeO_2 containing gels while only part of the alumina crystallizes as $LaAlO_3$ in the gels derived from $La[Al(OPr^i)_4]_3$.

The oxygen storage capacity and the catalytic behavior of Pt/Rh deposited on our $LaCeAl_{11}$ and $LaCeAl_{13}$ is under investigation and the results will be presented in a future publication.

The use of Bruker WM-360 NMR, Philips CM1 2/STEM analytical electron microscope, and PHI 5200 ESCA at University of Michigan, Ann Arbor is gratefully acknowledged. W. L. Watkins (Ford) provided BET surface area data. The authors thank D. Levin (M.I.T.) for technical assistance. This study was supported in part by National Science Foundation (CTS-9257223). The high-resolution transmission microscopy of the samples was sponsored by the Assistant Secretary for Energy and Renewable Energy, Office of Transportation Technologies, as part of the High Temperature Materials Laboratory Fellowship program, Oak Ridge National Laboratory, managed by Lockheed Martin Research Corp. for the US Department of Energy under contract number DE-AC05–96OR22464.

References

1 C. J. Brinker and G. W. Scherer, *Sol–Gel Science*, Academic Press, London, 1990.
2 L. C. Klein, *Sol–Gel Technology for Thin Films, Fibers, Preforms, Electronics, and Specialty Shapes*, Noyes Publications, New Jersey, USA, 1988.
3 J. Y. Ying, J. B. Benzinger and A. Navrotsky, *J. Am. Ceram. Soc*., 1993, **76,** 2571.
4 K. G. Caulton and L. G. Hubert-Pfalzgraf, *Chem. Rev*., 1990, **90**, 969.
5 L. G. Hubert-Pfalzgraf, *Polyhedron*, 1994, **13**, 1118.
6 D. C. Bradley, R. C. Mehrotra and D. P. Gaur, *Metal Alkoxides*, Academic Press, London, 1978.
7 C. K. Narula, *US Pat*., 5 134 107, 1992.
8 C. K. Narula, *Mater. Res. Soc. Symp. Proc*., 1992, **271,** 181.
9 R. C. Mehrotra, *Chemtracts Anal. Phys. Inorg. Chem*., 1990, **2**, 389.
10 K. Jones, T. J. Davies, H. G. Emblem and P. Parkes, *Mater. Res. Soc. Symp. Proc*., 1986, **73**, 111.
11 J. Rai and R. C. Mehrotra, *J. Non-Cryst. Solids*, 1993, **152**, 118.
12 J. Rai and R. C. Mehrotra, *J. Non-Cryst. Solids*, 1991, **134**, 23.
13 C. K. Narula, J. H. Visser and A. Admczyk, *US Pat*., 5 480 622, 1996.
14 C. K. Narula and A. Admczyk, *US Pat*., 5 431 012, 1995.
15 J. H. Visser, C. K. Narula and M. Zanini, *US Pat. Appl.*
16 C. K. Narula, H. Jen and H. S. Gandhi, *US Pat. Appl*., 08/311 298, Sept. 23, 1994.
17 C. K. Narula, W. L. H. Watkins and M. Shelef, *US Pat*., 5 210 062, 1993.
18 T. Miki, T. Ogawa, M. Haneda, N. Kakuta, A. Ueno, S. Tateishi, S. Matsura and M. Sato, *J. Phys. Chem*., 1990, **94**, 6464.
19 N. Watanabe, H. Yamashita, K. Akira, H. Kawagoe, S. Matsuda, *Jpn. Kokai Tokkyo Koho JP*, 63 175 642, 1988; *Chem. Abstr*., 1989, **110**, 64521.
20 H. C. Yao and Y. F. Yu-Yao, *J. Catal*., 1984, **86**, 254.
21 G. W. Graham, P. J. Schmitz, R. K. Usmen and R. W. McCabe, *Catal. Lett*., 1993, **17**, 175.
22 J. G. Nuna, H. J. Robota, M. J. Cohn and S. A. Bradley, *Catalysis and Automotive Pollution Control*, ed. A. Crucq, Elsevier, Amsterdam, 1991, vol. 2, p. 221.
23 R. C. Mehrotra, A. Singh and U. M. Tripathi, *Chem. Rev*., 1991, **91**, 1287.
24 R. C. Mehrotra, P. N. Kapoor and J. M. Batwara, *Coord. Chem. Rev*., 1980, **31**, 67.
25 R. C. Mehrotra and M. M. Agrawal, *Chem. Commun*., 1968, 469.
26 R. C. Mehrotra, M. M. Agrawal and A. Mehrotra, *Synth. Inorg. Metal-Org. Chem*., 1973, **3**, 181.
27 S. Hirano, T. Yogo, K. Kikuta, H. Urahata, Y. Isobe, T. Morishita, K. Ogiso and Y. Ito, *Mater. Res. Soc., Symp. Proc*., 1992, **271**, 331.
28 R. Kuhlman, B. A. Vaartstra, W. E. Streib, J. C. Hufman and K. G. Caulton, *Inorg. Chem*., 1993, **32**, 1272.
29 J.-F. Campion, D. A. Payne, H. K. Chae, J. K. Maurin and S. R. Wilson, *Inorg. Chem*., 1991, **30**, 3245.
30 J. B. Benzinger, S. J. McGovern and B. S. H. Royce, in *ACS Symp. Ser. No. 288, Catalyst Characterization Science*, ed. M. L. Deviney and J. L. Gland, ACS, Washington DC, 1985, pp. 449–463.
31 J. Y. Ying, J. B. Benzinger and H. Gleiter, *Phys. Rev. B*, 1993, **48**, 1830.
32 J. R. McBride, K. C. Hass, B. D. Poindexter and W. H. Weber, *J. Appl. Phys*., 1994, **76**, 2435.
33 E. Zintl and U. Croatto, *Z. Anorg. Allg. Chem*., 1939, **242**, 79.
34 G. W. Graham, W. H. Weber, C. R. Peters and R. Usmen, *J. Catal*., 1991, **130**, 310.
35 W. H. Weber, K. C. Hass and J. R. McBride, *Phys. Rev. B*, 1993, **48**, 178.
36 J. Z. Shyu, W. H. Weber and H. S. Gandhi, *J. Phys. Chem*., 1988, **92**, 4964.
37 L. P. Haack, J. E. de Vries, K. Otto and M. S. Chattha, *Appl. Catal. A*, 1992, **82**, 199.
38 J. S. Church, N. W. Cant and D. L. Trimm, *Appl. Catal. A*, 1993, **101**, 105.
39 C. D. Wagner, H. A. Six, W. T. Jansen and J. A. Taylor, *Appl. Surf. Sci*., 1981, **9**, 203.
40 R. P. Vasquez, *Surf. Sci. Spectra*, 1992, **1**, 361.
41 B. R. Strohmeier, D. E. Leyden, R. S. Field and D. M. Hercules, *J. Catal*., 1985, **94**, 514.
42 L. Salvati, Jr., L. E. Makovsky, J. M. Stencel, F. R. Brown and D. M. Hercules, *J. Phys. Chem*., 1981, **85**, 3700.
43 B. R. Strohmeier and D. M. Hercules, *J. Phys. Chem*., 1984, **88**, 4922.
44 Y. Uwamino and T. Isizuka, *J. Electron Spectrosc. Relat. Phenom*., 1984, **34,** 67.

Paper 7/02102J; *Received* 26*th March*, 1997